NUCLEAR THEORY, Vol. 31 (2012)
eds. A. Georgieva, N. Minkov, Heron Press, Sofia

Angular Anisotropy of the Fission Fragments in the Dinuclear System Model

T.M. Shneidman[1], **A.V. Andreev**[1], **M.T. Pigni**[2], **C. Massimi**[3,4], **G. Vannini**[3,4],**A. Ventura**[4,5]

[1]Bogoliubov Laboratory of Theoretical Physics, Joint Institute for Nuclear Research, 141980 Dubna, Russia

[3]Dipartimento di Fisica dell' Università di Bologna, 40126 Bologna, Italy

[4]INFN, Sezione di Bologna, 40126 Bologna, Italy

[5]ENEA, Centro Ricerche Ezio Clementel, 40129 Bologna, Italy

Abstract. A theoretical evaluation of the collective excitation spectra of nucleus at large deformations is possible within the framework of the dinuclear system (DNS) model, which treats the wave function of the fissioning nucleus as a superposition of a mononucleus configuration and two-cluster configurations in a dynamical way, permitting exchange of nucleons between clusters. In this work the method of calculation of the potential energy and the collective spectrum of fissioning nucleus at scission point is presented. Combining the DNS model calculations and the statistical model of fission we calculate the mass, total kinetic energy, and angular distribution of fission fragments for the neutron–induced fission of ^{239}Pu.

1 Introduction

During the last years an investigation of the cluster properties of heavy nuclei attracts more and more attention of the theoreticians and experimentalists working in nuclear physics. The first indications of an existence of sufficiently long living cluster-type configurations in heavy nuclear systems have been found in deep inelastic heavy ion collisions [1]. These cluster configurations composed of two touching fragments were called dinuclear systems (DNS). Later, the DNS concept was successfully applied to the description of the fusion process which was treated as the evolution of the initially formed DNS in mass asymmetry coordinate [2].

The cluster degrees of freedom play an important role in the fission process. It was shown, that the fissioning nucleus at the late stages of fission just before the separation of two primary fragments can be considered as a system of two interacting clusters [3]. This consideration has been used to calculate mass, total kinetic energy and angular momentum distributions of fission fragments in neutron induced and spontaneous fission of actinides [3, 4]. The shell model calculations [5] demostrated that the actinides in third minimum closely related to the system of two touching clusters (DNS), both in shape and in single particle structure. The arguments were presented that super- (SD) and hyperdeformed (HD) nuclear states can be considered as the DNS [6].

The evidences of cluster properties have been revealed also at ground state deformations of heavy nuclei. Strong correlation between the alpha-decay hindrance factor and energy of the lowest negative parity state in heavy alpha-emitters demonstrated in [7] leads to the conclusion that the reflection asymmetric deformation of these nuclei caused by the admixture of alpha-cluster configurations to the intrinsic nuclear wave function [8].

The above-mentioned examples show the importance of cluster features at various deformations of heavy nuclei. Thereby, in the fission process, where the deformation of fissioning nucleus changes from ground state to scission, the independent treatment of cluster degrees of freedom seems to be essential. The description which includes both the deformation and cluster degrees of freedom is provided by the DNS model.

In the present work we discuss the application of the DNS model to fission process and apply the model to calculate mass distribution, mean value of total kinetic energy and angular anisotropy of the fragments produced in neutron–induced fission of ^{239}Pu.

2 Fission in the Dinuclear System Model

Instead of parametrizing the shape of the fissioning nucleus in terms of multipole deformation parameters β_0, β_1, β_2, β_3, ..., the dinuclear system model (DNS) deals with degrees of freedom related to the dinuclear system. Under the expression dinuclear system we understand the system of two touching fragments (A_1,Z_1) and (A_2,Z_2) with $A_1 + A_2 = A$ and $Z_1 + Z_2 = Z$ kept together by the molecular–type nucleus–nucleus potential. The special case of the dinuclear system in which one fragment has zero mass is denoted as a mononucleus.

Each dinuclear system configuration can be specified by the mass-asymmetry $\xi = 2A_2/A$, charge-asymmetry $\xi_Z = 2Z_2/Z$ and the vector of the relative distance $\mathbf{R} = (R, \theta_R, \phi_R)$. The values ξ = 0 or ξ = 2 correspond to the mononucleus configurations ($A_1 = A, A_2 = 0$) or ($A_1 = 0, A_2 = A$), respectively. Each fragment of DNS is characterized by the quadrupole deformation parameters (β_i, γ_i), $(i = 1, 2)$ and the set of Euler angles $\Omega_i = (\phi_i, \theta_i, \alpha_i)$, $(i = 1, 2)$ describing orientation of the fragments in the laboratory frame. These give a total of 15 degrees of freedom, which can be used to describe the collective motion in a dinuclear system consisting of quadrupole-deformed fragments.

The main idea of the DNS model is that neither a single mononucleus nor a single dinuclear system can alone describe the nucleus. The intrinsic nuclear wave function can rather be described as a superposition of the mononucleus and different dinuclear configurations. The mononucleus is taken to be quadrupole-deformed; thus, in the DNS model, the contribution to the reflection asymmetric deformation of the nucleus related solely to the nonzero weight of the asymmetric dinuclear systems. This choice of the nuclear wave function gives us the possibility to describe in one approach the ground state properties of heavy nuclei and the fission process as well. The various stages of fission can be characterized by the major contribution of different dinuclear systems to the total wave function of nucleus.

Qualitatively, when a nucleus is moving along the fission barrier, the elongation of the nuclear system increases. The increase of the elongation of the dinuclear systems that contribute to the nuclear wave function can be achieved either by increase of the deformations of DNS fragments or by increase of mass asymmetry. As shown in Ref. [8], in the vicinity of the ground state the nuclear wave function can be roughly represented as a superposition of a mononucleus and a DNS with an alpha particle as the light cluster ($\xi = \xi_\alpha$). The contribution of DNS with $\xi > \xi_\alpha$ is negligible due to the much larger potential energies of such systems or due to the huge barrier separating these systems from the ground state. Our calculations have shown that the increase of elongation of the fissioning nucleus up to the saddle-point is achieved mainly by the increase of deformation of the heavy DNS fragments (and the mononucleus) while $\xi \le \xi_\alpha$ [9].

After passing the second saddle point the increase of elongation of the fissioning nucleus is related mostly to the rapid increase of the contribution of DNS's with $\xi_\alpha \le \xi \le 1$ while the contribution of the mononucleus configuration vanishes. Simultaneously, the dinuclear system characterized by the mass asymmetry ξ has the possibility of decaying in relative distance coordinate R and undergoing fission. The competition between these two processes determines the dynamics of the fissioning nucleus beyond the saddle point.

As a first step towards the solution of these problems, in this work we consider the limiting case of a well defined scission configuration, assuming that statistical equilibrium among various degrees of freedom of the system is established before the decay in R [3]. It is thus possible to calculate the probabilities of different scission point configurations, and, consequently, to describe various fission characteristics, such as mass and charge yields as well as kinetic-energy and angular distributions of fission fragments.

3 Potential Energy and Relative Yields at Scission

The fissioning nucleus at scission point is considered as a system of two axially–deformed fragments (A_1, Z_1) and (A_2, Z_2). Under the assumption of a small overlap of nuclei in the dinuclear system, the potential energy of the DNS model is calculated as the sum of the binding energies of the fragments B_i, $(i = 1, 2)$ and the interaction V^{int} between the fragments [3]

$$\begin{aligned} U(\xi, \xi_Z, \beta_i, \gamma_i, \Omega_i, R_i, \{i = 1, 2\}) \\ = B_1(A_1, Z_1, \beta_1, \gamma_1) + B_2(A_2, Z_2, \beta_2, \gamma_2) \\ + U^{int}(\xi, \xi_Z, R, \beta_i, \gamma_i, \Omega_i, R_i, \{i = 1, 2\}). \end{aligned} \quad (1)$$

This approach allows us to calculate the potential energy as a function of the DNS degrees of freedom: mass and charge asymmetries ξ and ξ_Z, internuclear distance R, deformation parameters β_i and orientation angles Ω_i of the fragments ($i = 1, 2$).

The binding energy of the fragment (A_i, Z_i) with deformation β_i is calculated as the sum of the liquid drop energy U_i^{LD} and the shell correction term δU_i^{shell}

$$B_i = U_i^{LD} + \delta U_i^{shell}, \qquad (i = 1, 2). \tag{2}$$

The liquid drop energy is calculated using the parameters that give, together with shell corrections, the best fit to the experimental binding energies of the separate fragments at their ground-state deformations [3]. The deformation-dependent shell corrections are calculated with the two-center shell model (TCSHM) [10]. The TCSHM can not be directly used to calculate the shell-correction term for the whole binary system. Due to the fact that the TCSHM describes the binary system as a strongly deformed nucleus, the neutron-to-proton ratio N/Z is the same in different parts of the binary system and it is not possible to set the masses and charges of the fragments separately. To avoid this difficulty, we calculate the shell-correction terms separately for each fragment using the following method. For the fragment, (A_i, Z_i) with deformation parameter β_i, we consider a symmetric binary system $(A_i, Z_i) + (A_i, Z_i)$ with well separated equally deformed fragments. Then the half of the obtained value of the shell correction is taken as a shell correction of one fragment.

The interaction energy, U^{int}, is calculated as a sum of the Coulomb U^C and nuclear U^N interactions. The latter is taken in the form of a double folding of nuclear densities and density-dependent Skyrme-type nucleon-nucleon forces [11].

The nuclear part of the interaction energy is attractive for $R > R_1 + R_2 - a$ and repulsive for $R > R_1 + R_2 - a$, where $a \approx 1.5$ fm, thus simulating the Pauli principle and the structure forbiddeness effects in the motion to smaller values of R. As a result of the interplay between nuclear and Coulomb interaction, the interaction potential U^{int} can have a potential pocket corresponding to the pole-to-pole configuration of nearly touching fragments. The depth and the position of this pocket depends on the masses and deformations of the fragments of the dinuclear system. For asymmetric dinuclear systems corresponding to actinides the minimum of the potential pocket is located at the touching distances. For nearly symmetric dinuclear systems, depending on fragment deformations, the minimum of U^{int} is shifted to distances (0.5 – 1) fm larger than the touching distance. The existence of the minimum of the potential energy of the dinuclear system at distances equal or larger than the touching one justifies the expression (1) for the potential energy used in the DNS model.

To obtain observable quantities of fission we assume that the barrier in relative distance R keep the nuclei of DNS in contact for some time with the consequence that the fissioning nucleus take a statistical distribution in the potential surface. Then the relative probability that the fissioning nucleus at scission can be in the form of the DNS whose fragments have mass and charge numbers (A_1, Z_1) and (A_2, Z_2) and deformations β_1 and β_2 can be written as

$$P(\{A_i, Z_i, \beta_i\}, R_b) = P_0 \exp\left(-\frac{U(\{A_i, Z_i, \beta_i\}, R_b)}{T}\right), \qquad (3)$$

where T is the temperature related to the excitation energy $T = (E^*/a)^{1/2}$ and $a = A/12$ MeV^{-1}, with A the mass number of the fissioning nucleus. The scission point is at nuclear distance $R = R_b$, with R_b denotes the position of the outer barrier in relative distance between the fragments. The potential energy in (3) is calculated by means of eq.(1) for the pole–to–pole configuration which corresponds to the minimum of the potential energy. The damping of shell corrections with excitation energy is taken into account in calculations of the binding energies of the fragments. The results of calculations are presented in Figure 1 for the splittings ^{240}Pu→^{96}Sr+^{144}Ba and ^{240}Pu→^{102}Zr+^{138}Xe.

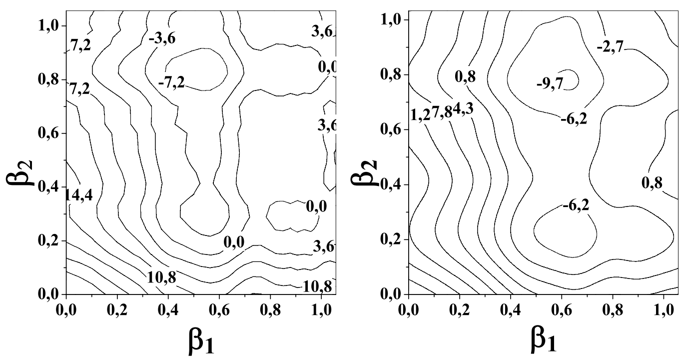

Figure 1. Potential Energies (in MeV) of the scission configurations for the neutron–induced fission of ^{240}Pu leading to the ^{96}Sr+^{144}Ba (left) and ^{102}Zr+^{138}Xe (right) primary fragments. The potential energies are calculated with respect to the ground state energy of ^{240}Pu.The deformations of lighter (heavier) fragments of DNS are denoted as β_1 (β_2).

The expression (3) is used to obtain the mass distribution of primary fission fragments (before evaporation of neutrons)

$$Y(A_1) \sim \sum_{Z_1} \int \exp\left[-\frac{U(\{A_i, Z_i, \beta_i\}, R_b)}{T}\right] \mathrm{d}\beta_1 \mathrm{d}\beta_2. \qquad (4)$$

Figure 2 shows results of calculations of mass distribution for thermal-neutron induced fission of ^{239}Pu in good agreement with experimental data.

The important characteristic of fission is the kinetic energy of fission fragments. In the present work it is supposed that all the interaction energy of the

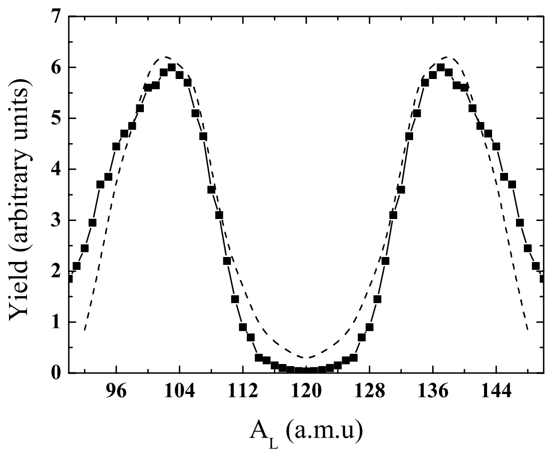

Figure 2. Fragment mass distribution for thermal-neutron induced fission of ^{239}Pu. Dashed line: calculation in the scission point model. Points connected by the solid line as an eye guide: experimental (pre-neutron emission) mass yields given by Ref. [12].

system at scission transforms after fission to the kinetic energy of the fragments:

$$\mathrm{TKE} = V^{C,int} + V^{N,int}, \tag{5}$$

where TKE is the total kinetic energy of the fragments. This method assumes no pre-scission kinetic energy in the system. If one introduces it to the model, the values of TKE can increase by several MeV.

The distribution of the total kinetic energy for fixed masses of the fragments is smoothed. Usually the main characteristics of this distribution, the mean TKE of the fission fragments and variation of TKE, are measured. In the statistical approach the mean total kinetic energy of the fragments for the fission of a particular binary system can be calculated using the following expression:

$$\langle \mathrm{TKE} \rangle > (A_1, Z_1, A_2, Z_2) = \frac{\iint \mathrm{TKE}(\{A_i, Z_i, \beta_i\}) \exp[-U(\{A_i, Z_i, \beta_i\})/T] \mathrm{d}\beta_1 \mathrm{d}\beta_2}{\int\int \exp[-U(\{A_i, Z_i, \beta_i\})/T] \mathrm{d}\beta_1 \mathrm{d}\beta_2}. \tag{6}$$

This formula uses the probabilities of different configurations to calculate the mean value of TKE. Hence, one should take the potential energy U calculated at the barrier of the interaction potential. The results of the calculation for the neutron–induced fission of ^{239}Pu are presented on Figure 3.

4 Angular Distribution of the Fission Fragments

Using the Boltzmann factor given by formula (3) we can calculate mean values of fragment masses A_H and A_L, with $A_H + A_L = A$, and corresponding

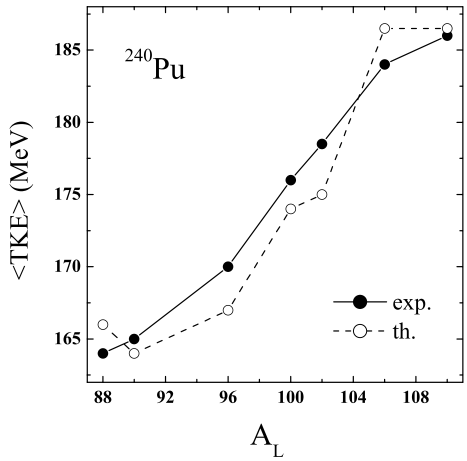

Figure 3. Comparison of calculated and experimental average kinetic energy of fragments for neutron-induced fission of ^{239}Pu as functions of the mass number of the light fragment, from [3].

fragments's deformations β_H and β_L. These determine the most favourable dinuclear configuration at the scission point. If the fissioning nucleus has total angular momentum J and J-projection M on the direction of the incident neutron beam, it is possible to determine a set of states with quantum numbers J and M that related to the excitation of different rotational and vibrational degrees of freedom of the most favourable dinuclear configuration. In particular, the rotational degrees of freedom correspond to the independent rotations of the two fragments and to the rotation of the DNS as a whole. In the past, similar techniques have been used for the calculation of angular momentum distribution of fission fragments [4, 13].

The Hamiltonian describing the collective excitations of the DNS consisting of fragment (A_H, Z_H) with deformation β_H, and fragment (A_L, Z_L) with deformation β_L can be written as:

$$\begin{aligned}\hat{H} =& \frac{\hbar^2\left(\hat{J}_H^2 - \hat{J}_{H,(3)}^2\right)}{2\Im_H^{\perp}} + \frac{\hbar^2\hat{J}_{H,(3)}^2}{2\Im_H^{||}} \\ &+ \frac{\hbar^2\left(\hat{J}_L^2 - \hat{J}_{L,(3)}^2\right)}{2\Im_L^{\perp}} + \frac{\hbar^2\hat{J}_{L,(3)}^2}{2\Im_L^{||}} \\ &+ \frac{\hbar^2\hat{J}_0^2}{2\Im_0} + U(\Omega_1, \Omega_2), \end{aligned} \tag{7}$$

where $U(\Omega_0, \Omega_1, \Omega_2)$ is the potential energy of the dinuclear system as a function of the relative orientation of fragments, $\hat{J}_H$ ($\hat{J}_{H,(3)}$), $\hat{J}_L$ ($\hat{J}_{L,(3)}$), and $\hat{J}_0$ are the angular momenta (and their projections on the DNS symmetry axis) of the two fragments and the relative angular momentum, respectively. The relative moment of inertia of the system is denoted as $\Im_0$. The quantities $\Im_H^{\perp}$ ($\Im_H^{||}$), $\Im_L^{\perp}$ ($\Im_L^{||}$) are the perpedicular (parallel) moments of inertia of the corresponding fragments calculated in the rigid body limit. The choice of rigid body moments of inertia are justified since the dinuclear system at the scission point is highly excited.

In order to simplify the eigenvalue problem for the Hamiltonian (7) we approximate the potential energy by the expansion

$$\begin{aligned} &U(\{\epsilon_1,\delta_1\},\{\epsilon_2,\delta_2\}) \\ &\quad = u_0 + \frac{c_1}{2}\sin^2\epsilon_1 + \frac{c_2}{2}\sin^2\epsilon_2 + c_{12}\sin 2\epsilon_1 \sin 2\epsilon_2 \cos(\delta_1-\delta_2), \end{aligned} \quad (8)$$

where (ϵ_i, δ_i), $i = (1,2)$ are the Euler angles describing, respectively, the orientation of the fragments A_L and A_H in the molecular coordinate system, connected with vector $\mathbf{R_m}$. The similar expansion was used previously in [14] for the description of high–spin heavy–ion resonances. Expressing angles (ϵ_i, δ_i), (i=1,2) in laboratory frame we obtain

$$\begin{aligned} &U(\Omega_0,\Omega_L,\Omega_H) \\ &\quad = U_0 + \frac{C_L}{2}\left[Y_2(\Omega_0)\times Y_2(\Omega_L)\right]_{(00)} + \frac{C_H}{2}\left[Y_2(\Omega_0)\times Y_2(\Omega_H)\right]_{(00)} \\ &\qquad - C_{hl}\sum_{L=0,2,4} C^{L0}_{21,\,2-1}\left[Y_L(\Omega_0)\times\left[Y_2(\Omega_L)\times Y_2(\Omega_H)\right]_L\right]_{(00)}. \end{aligned} \quad (9)$$

Coefficients C_H, C_L and C_{hl} entering the expression (9) are fixed by fitting the angular dependence of the potential energy calculated with use of Eq.(1).

Diagonalizing the Hamiltonian (7) we obtain its eigenvalues $E^{n,K_H,K_L}_{JM\Pi}$ as well as its eigenfunctions, $\Psi^{n,K_H,K_L}_{JM\Pi}(\Omega_H,\Omega_L,\Omega_0)$. Assuming that the decay of the scission-point configuration is a fast process, the probability of emitting fission fragments from the state $\Psi^n_{JM\Pi}$ at an angle θ is given by:

$$P^{n,K_H,K_L}_{JM\Pi} = \sin\theta d\theta \int |\Psi^{n,K_H,K_L}_{JM\Pi}|^2 d\Omega_H d\Omega_L d\phi \quad (10)$$

Here, the change of the angular distribution caused by the Coulomb excitation subsequent to the fission is neglected.

The angular distribution of fission fragments for the channel characterized by angular momentum J, projection M, parity Π at temperature T can be written as

$$W_{JM\Pi}(E^*,\theta) = A(J)\sum_{n,K_H,K_L}\exp\left[-\frac{E^{n,K_H,K_L}_{JM\Pi}}{T(E^*)}\right] P^{n,K_H,K_L}_{JM\Pi}, \quad (11)$$

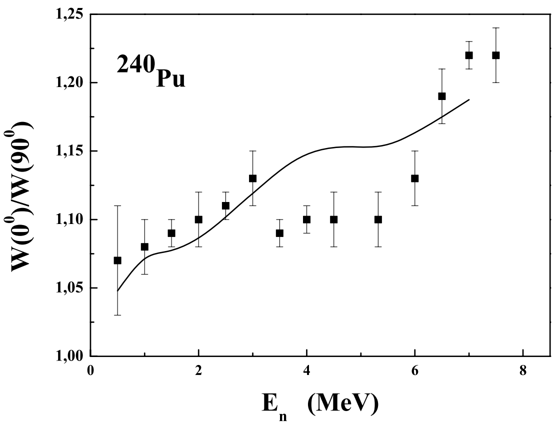

Figure 4. Calculated and experimental angular anisotropy of fission fragments vs incident neutron energy. Data are taken from Ref. [15].

with $A(J)$ a normalization constant.

Summing over the contributions of different channels, it is possible to compute the total angular distribution, $W(\theta)$; a quantity that is commonly compared with experimental data is the angular anisotropy, $W(\theta = 0)/W(\theta = \pi/2)$, evaluated as a function of E_n, as shown in Figure 4.

Our theoretical results are in good agreement with experimental data at low energies ($E_n < 4$ MeV) . The behaviour at higher energies, where the experimental angular anisotropy first decreases and then rapidly increases again above 6 MeV may be due to the interplay of two factors that are not yet included in our model. The decrease of the angular anisotropy may be related to the threshold of excitation of two-quasi-particle states in the fragments of the most favourable dinuclear configuration. The rapid increase above 6 MeV energy is associated with the threshold of second-chance fission [16]. The amount of angular momentum carried away by the evaporated neutron is small compared with the angular momentum of the compound system. However, the excitation energy is significant and, as a result, the angular anisotropy decreases.

5 Conclusion

In the present work we have discussed the application of the dinuclear system model to the fission process. The key idea of our approach is the account taken of the cluster degrees of freedom related to the formation of the DNS. Combining the DNS model with the scission-point model, we have computed mass distributions, mean total kinetic energy and angular anisotropies of fission fragments in neutron-induced fission of ^{239}Pu. The results are in good agreement with experiments. The calculations for angular anisotropies can be improved by including the effects of non-collective states and second-chance fission.

References

[1] V.V. Volkov, *Izv. Akad. Nauk SSSR, Ser. Fiz.* **50** (1986) 1879.
[2] G.G. Adamian, *et al.*, *Nucl. Phys*. **A633** (1998) 409.
[3] A.V. Andreev, *et al.*, *Eur. Phys*. **A26** (2005) 327.
[4] T.M. Shneidman, *et al.*, *Phys. Rev. C* **65** (2002) 064302.
[5] S. Cwiok, *et al.*, *Phys. Lett. B* **322** (1994) 304.
[6] T.M. Shneidman *et al.*, *Nucl. Phys.* **A671** (2000) 119.
[7] R.K. Sheline and M.A. Riley, *Phys. Rev. C* **61** (2000) 057301.
[8] T.M. Shneidman, *et al.*, *Phys. Lett. B* **526** (2002) 322.
[9] T.M. Shneidman, A.V. Andreev, M.T. Pigni, C. Massimi, G. Vannini, A. Ventura, EPJ Web of Conference, to be published in 2012.
[10] J. Maruhn and W. Greiner, *Z. Physik* **251** (1972) 431.
[11] G.G. Adamian, *et al.*, *Int. J. Mod. Phys*. **E5** (1996) 191.
[12] C. Wagemans *et al.*, *Phys. Rev. C* **30**, (1984) 218.
[13] M. Zielinska-Pfabe' and K. Dietrich, *Phys. Lett B*. **49** (1974) 123.
[14] E. Uegaki and Y. Abe, *Prog. Theor. Part. Phys.* **90** (1993) 615.
[15] J.E. Simmons and R.L. Henkel, *Phys. Rev*. **120**, (1965) 198; R.B. Leachman and L. Blumberg, *Phys. Rev. B* **137**, (1965) 814.
[16] R. Vandenbosch, J.R. Huizenga, "*Nuclear Fission*" (Academic Press, New York and London, 1973).